Pseudospin Kondo correlations versus hybridized molecular states in double quantum dots

A. W. Holleitner,[1,*] A. Chudnovskiy,[2] D. Pfannkuche,[2] K. Eberl,[3] and R. H. Blick[4]
[1]*Center for NanoScience (CeNS), LMU Munich, Geschwister-Scholl-Platz 1, 80539 Munich, Germany*
[2]*I. Institut für Theoretische Physik, Hamburg University, Jungiusstrasse 9, 20355 Hamburg, Germany*
[3]*Max-Planck-Institut für Festkörperforschung, 70569 Stuttgart, Germany*
[4]*Electrical and Computer Engineering, University of Wisconsin-Madison, Madison, Wisconsin 53706-1691, USA*
(Received 21 January 2004; published 10 August 2004)

A double quantum dot is coupled in parallel for studying the competition between the pseudospin Kondo correlations and strongly hybridized molecular states. Cryogenic measurements are performed in the regime of weak coupling of the two dots to leads under linear transport conditions. A detailed theoretical model is presented which verifies the finding of the transition between the two different regimes.

DOI: 10.1103/PhysRevB.70.075204 PACS number(s): 73.63.Kv, 72.10.Fk, 73.23.−b

INTRODUCTION

The Kondo problem elucidates the interplay between localized quantum states and delocalized mediating wave functions.[1–3] Many aspects of the physics involved can by now be tested using quantum dots which act as Kondo impurities at very low temperatures.[4–7] Correlations between quantum states of delocalized lead electrons and localized electrons of a single quantum dot generate a resonant second-order tunneling of electrons that screens the local spin of the quantum dot. Expanding the dot system by defining two coupled quantum dots, the orbital structure of the wave functions acquires spinlike features which can be expressed in terms of a pseudospin. Previous theoretical work predicted the existence of this SU(4) pseudospin Kondo effect in double quantum dots for efficiently strong interdot Coulomb interactions.[8] Here we realize such a double quantum dot and show that the pseudospin Kondo correlations can be detected in transport by coupling the dots in parallel to source and drain contacts.[9] We find an extra resonance in the conductance through the device when the ground-state energy of the double quantum dot is unchanged by the transfer of an electron between the two single quantum dots. We show that unlike the spin Kondo effect this resonance is insensitive to an external magnetic field of up to 2 T. Based upon the concept of pseudospin, we derive an expression for the first- and second-order electron tunneling through the parallel double quantum dot. Comparison between the model and data demonstrates that the conductance resonance is due to pseudospin Kondo correlations. The two degenerate states with one electron being in either of the two quantum dots play the role of pseudo-spin-up and pseudo-spin-down states. The resonant enhancement of the conductance occurs in the regime where the single-particle tunneling between the double dot and adjacent leads is blocked. Moreover, the interdot tunneling t breaks the pseudospin Kondo correlations in the same way as an external magnetic field does for the real spin Kondo effect. At very large tunneling, the states with an electron on either quantum dot are strongly hybridized and form a molecular ground state.[10] In that state, the pseudospin is frozen in the symmetrical combination of pseudospin-up and pseudospin-down directions. Thus, the pseudospin Kondo effect and second-order tunneling through the double quantum dot are suppressed. The experiment shows this transition in agreement with the theoretical model.

EXPERIMENT

The double quantum dot is defined in a two-dimensional electron system (2DES) via the biasing of Schottky gates patterned on top of an AlGaAs/GaAs heterostructure. The sheet electron density and mobility of the 2DES, which is 90 nm below the surface, are found to be $\mu = 80\ \mathrm{m}^2/\mathrm{V\,s}$ and $n_S = 1.7 \times 10^{15}\ \mathrm{m}^{-2}$ at 4.2 K. As depicted in Fig. 1(a) and explicitly described in Refs. 11–13 the two dots are built in

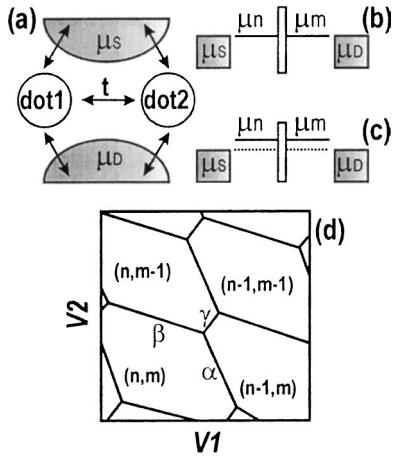

FIG. 1. (a) Parallel double quantum dot with each dot connected to source and drain with the chemical potentials μ_S, μ_D. The interdot tunnel coupling is denoted by t. (b) Resonant first-order level scheme in relative energy ε: the chemical potentials μ_n and μ_m [for $n(m)$ electrons being on $\mathrm{dot}_1(\mathrm{dot}_2)$] are aligned to the chemical potentials of the leads. The open box depicts the interdot tunneling barrier. (c) For levels being off resonant the resonant state generated by correlated tunneling processes (dashed line) at the Fermi level can be detected. In this configuration the phase transition between first- and second-order tunneling is traced. (d) Schematic phase diagram of a double quantum dot in response to two gate voltages $V1$ and $V2$: black lines illustrate phase boundaries α, β, and γ between two ground-state configurations.

an Aharonov-Bohm geometry with tunable interdot tunneling t by a two-step electron beam writing process. In this geometry it is possible to measure correlated second-order tunnel events (cotunneling) not only for the chemical potentials of both dots being aligned to the Fermi levels μ_S and μ_D of source and drain [see Fig. 1(b)], but also for the off-resonant condition sketched in Fig. 1(c). In order to characterize the coupled quantum dots we measure the conductance from source to drain while sweeping the chemical potentials of the two dots separately. This is achieved by two electrostatically coupled top gates; i.e., we apply two voltages V_1 and V_2 for dot_1 and dot_2, respectively.[13–16] For coupled double dots this leads to phase diagrams with hexagonal patterns as depicted in Fig. 1(d).[13] In the diagram each line indicates the phase boundary between two ground states with a fixed electron number in the double quantum dot. For lines parallel to α (β) the chemical potential of dot_1 (dot_2) is aligned to source and drain. Consequently, single electrons are tunneling via this dot and the corresponding electron number is reduced by one—e.g., from n to $n-1$ (m to $m-1$). This sequential tunneling is well described by the orthodox theory.[17] A very distinct feature is given by line γ which refers to Fig. 1(c). At these energetic configurations two electrons can resonantly tunnel through the parallel-double-dot system,[9] and the transition from a delocalized pseudospin Kondo state to a localized ground state with a frozen pseudospin is detectable.

MEASUREMENTS

In order to verify this transition, we perform cryogenic transport spectroscopy on the parallel double quantum dot. The base temperature of the ^{3}He/^{4}He dilution refrigerator is $T_{bath}=55$ mK while the lock-in excitation is $V_{ac}=10$ μV at 17 Hz. The two measured quantum dots reveal charging energies of $E_1=e^2/C_1\sim 2.22$ meV (C_1 describes the total capacitance of dot_1) and $E_2\sim 2.76$ meV with single level spacings of about $\varepsilon_S\sim 240$ μeV. The gray scale plot in Fig. 2(a) depicts differential conductance measurements at zero bias voltage in reference to the two gate voltages V_1 and V_2. A comparison to Fig. 1(d) shows that only tunneling processes along line γ are resonant. The maximum conductance is of the order of $G=0.1e^2/h$. Since the conductance along lines α and β is below the noise level of about $\Delta G\sim 0.002e^2/h$, it follows that first-order tunneling through the quantum dots individually is suppressed. We note that the characteristic feature of the phase diagram—i.e., a finite conductance along line γ and no conductance along lines α and β—is continuously detectable up to a perpendicular magnetic field of $H\sim 2$ T [see, e.g., Fig. 2(b) for $H=1.5$ T]. By this, we can exclude both a spin-1/2 and a spin-1 Kondo effect being responsible for the cotunneling processes. At linear bias, an underlying spin-1/2 Kondo effect just would explain electron cotunneling close to zero magnetic field.[4–7] At the same time, a nontrivial orbital configuration with spin larger than 1/2 is only favorable for a finite range of magnetic field.[18] Instead, we find a robust homogeneous conductance along line γ throughout the sweeps. Only for the highest magnetic fields $H\sim 2$ T are the dot wave functions spatially compressed and the tunneling amplitudes to source and drain eventually lowered.

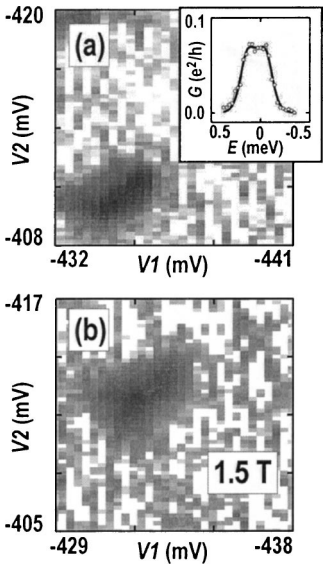

FIG. 2. (a) Pseudospin Kondo regime: logarithmic gray scale plot of a measured phase diagram (white $\leqslant 0$, $0.1e^2/h\leqslant$ black). Only second-order tunneling processes occur along the degenerate phase boundary between dot configurations $(n,m-1)$ and $(n-1,m)$. The inset depicts the comparison of the model (solid line) to experimental data (open circles) along line γ. (b) Equivalent phase diagram at a perpendicular magnetic field of 1.5 T.

THEORY

In the following we develop an expression for the conductance along line γ. Our derivation is based upon the idea that the electronic states in the double quantum dot form a so-called pseudospin.[8] The four states of the double-dot system which are involved in the transport along line γ are (n,m), $(n-1,m)$, $(n,m-1)$, and $(n-1,m-1)$ [see Fig. 1(d)]. In the absence of interdot tunneling t the ground-state energies of the two configurations $(n-1,m)$ and $(n,m-1)$ are equal along the line γ. The interdot tunneling leads to the mixing of the wave functions and splitting of the otherwise degenerate eigenenergies. The new eigenstates that we denote as pseudospin-up and pseudospin-down states are the symmetric and antisymmetric combinations of the states $(n-1,m)$ and $(n,m-1)$, $|\uparrow\rangle,|\downarrow\rangle=1/\sqrt{2}[(n,m-1)\pm(n-1,m)]$ with energies $\varepsilon_{\uparrow,\downarrow}=E(n,m-1)\pm t$. These two states constitute the low-energy sector of the model. The high-energy sector is given by the states $(n-1,m-1)$ and (n,m). Since in the middle of line γ the energy $E(n-1,m-1)$ is high with respect to the chemical potentials in the leads, $(n-1,m-1)$ is associated with an empty state. We introduce the fermion creation operators $\hat{c}_\uparrow^\dagger=|\uparrow\rangle\langle n-1,m-1|+|n,m\rangle\langle\downarrow|$ and $\hat{c}_\downarrow^\dagger=|\downarrow\rangle\langle n-1,m-1|-|n,m\rangle\langle\uparrow|$. Then the Hamiltonian of the isolated double-dot system reads

$$H_{dot}=\sum_{\sigma=\uparrow,\downarrow}[E(n,m-1)-E(n-1,m-1)]\hat{n}_\sigma + [E(n,m)-E(n,m-1)]\hat{n}_\uparrow\hat{n}_\downarrow + t(\hat{n}_\uparrow-\hat{n}_\downarrow), \quad (1)$$

with $\hat{n}_\sigma=\hat{c}_\sigma^\dagger\hat{c}_\sigma$. As motivated above, spin Kondo correlations

are not considered here; the subscript σ relates to the pseudospin. The tunneling between the leads and double dot is described by the Hamiltonian $H_{tun}=\Sigma_k\Sigma_{\nu=r,l}\Sigma_\sigma\{T^\nu_{k\sigma}\hat{a}^\dagger_{\nu k}\hat{c}_\sigma + \text{H.c.}\}$, where $\nu=r,l$ relates to the right and left leads, respectively. The creation of an electron in the lead ν with wave vector k is represented by $\hat{a}^\dagger_{\nu k}$. Note that the spin index of electrons in reservoirs is suppressed and that the tunneling is assumed to be spin independent. However, for a given mode (ν,k) the tunneling to the state with pseudospin up differs from the tunneling to the state with pseudospin down. The total Hamiltonian $H=H_{dot}+H_{tun}$ is similar to the Anderson impurity model with Zeemann field $t=(\varepsilon_\uparrow-\varepsilon_\downarrow)/2$. Performing the Schrieffer-Wolff transformation the effective pseudospin Kondo Hamiltonian reads

$$H_{pK}=\sum_{\nu\nu'}\sum_{kk'}\sum_{\mu=x,y,z}J^\mu_{\nu\nu'}(k,k')\hat{s}_\mu\hat{a}^\dagger_{\nu,k}\hat{a}_{\nu',k'}+t\cdot\hat{s}_z, \qquad (2)$$

where the Pauli matrix in the pseudospin space is denoted as $\hat{s}_\mu$. The actual value of the interdot tunneling t is renormalized by the tunneling to the leads. However, at small tunneling to the leads, which is the case in the experiment, the renormalization of t is small; hence, we neglect it. The asymmetry of the tunneling of each mode in the reservoir to different dots leads to the wave vector dependence of the pseudospin Kondo constants. In the case of the highest possible asymmetry—i.e., an electron coming from one of the reservoirs tunnels either to quantum dot 1 or to quantum dot 2—the modes of the reservoirs can be assigned with a pseudospin (orbital) index that remains conserved by tunneling. In that case the pseudospin Kondo effect is most pronounced. Even in the absence of the complete asymmetry the pseudospin Kondo couplings do not vanish, thus implying the existence of pseudospin Kondo correlations. The pseudospin Kondo constants vanish only for the completely symmetric tunneling of each mode to both dots. We calculated the two-particle cotunneling contribution to the current through the double quantum dot, which is a precursor of the pseudospin Kondo effect using Hamiltonian (2). We leave the question of the development of the pseudospin Kondo ground state for a future publication (see also Ref. 8). We obtain the contribution of the cotunneling in the form

$$I_{\text{cot}}=\Gamma_{\text{cot}}[F_B(\varepsilon_\uparrow)+F_B(\varepsilon_\downarrow)], \qquad (3)$$

where the Boltzmann distribution $F_B(\varepsilon)$ ensures that the state with energy ε is occupied. The cotunneling rate is given by

$$\Gamma_{\text{cot}}=\frac{1}{\{\ln[\max(T,t)/T_K]\}^2}\times\left[eV\frac{\sinh(2\beta t)\tanh(\beta t)[\cosh(\beta eV)-1]}{[\cosh(2\beta t)-1][\cosh(\beta eV)-\cosh(2\beta t)]}+2t\tanh(\beta t)\frac{\cosh(\beta eV)-\exp(-\beta eV)}{\cosh(2\beta t)-\cosh(\beta eV)}\right], \qquad (4)$$

with pseudospin Kondo temperature T_K and thermal energy $\beta=k_BT$ (k_B the Boltzmann constant). Without the interdot tunneling $t=0$ the cotunneling current is given by $I_{\text{cot}}\propto V/\{\ln[\max(T,t)/T_K]\}^2$, whereas the current gets exponentially suppressed with interdot tunneling at $2\beta t>1$, $I_{\text{cot}}\propto 2V/\{\ln[\max(T,t)/T_K]\}^2\beta te^{-2\beta t}$. The conductance of the double dot between the two triple points is given by the sum of the contribution from the sequential tunneling σ_{seq} that is parametrized by the sequential tunneling rate Γ_S (Ref. 19) and the cotunneling contribution $\sigma_{\text{cot}}=dI_{\text{cot}}/dV|_{V=0}$ that is obtained by differentiating Eq. (3). Now the expression $\sigma=\sigma_{seq}+\sigma_{\text{cot}}$ describes the experimental data in Fig. 2(a) along line γ. The fit parameters are the sequential tunneling rate Γ_S, the cotunneling rate Γ_{cot}, the ground-state energies of the isolated dots $E(n-1,m-1)$, $E(n,m-1)=E(n-1,m)$, $E(n,m)$, and the interdot tunneling amplitude t that simultaneously plays the role of Zeemann field for the pseudospin and the temperature T.

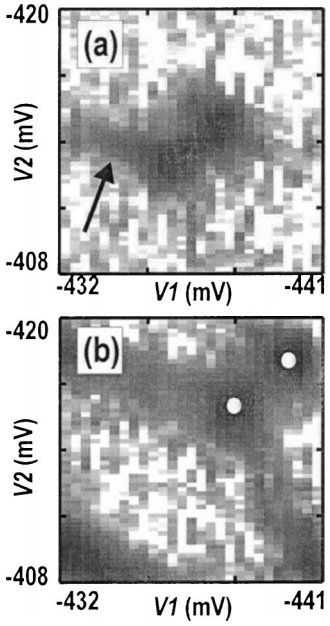

FIG. 3. (a) Phase transition: in addition to second-order processes, first-order processes (e.g. black arrow) are detectable (white $\leqslant 0$, $0.1e^2/h\leqslant$ black). (b) State with frozen pseudospin: along all phase boundaries only first-order processes can be traced. The white circles denote triple points where three charge configurations are degenerate.

DISCUSSION

The inset in Fig. 2(a) shows the comparison between the data along line γ and the fit with dot energies which equals the experimentally extracted ones. Confirming that in this regime the conductance is governed by cotunneling, the fit yields tunneling rates of $\Gamma_S=(284\pm8)$ MHz and $\Gamma_{\text{cot}}=(3.33\pm0.02)$ GHz. Using σ_{cot} alone, the fit yields a temperature reduced by about 40% which coincides with the difference between the bath temperature $T_{bath}=55$ mK and the electron temperature in the leads $T=(95\pm20)$ mK (Ref. 20) (see also Ref. 9). Figures 3(a) and 3(b) demonstrate the effect of increasing the interdot coupling.[11] In Fig. 3(a) the two dots exhibit pseudospin Kondo correlations along line γ. At the same time sequential tunneling processes contribute to the transport as indicated by the black arrow. Therefore, this

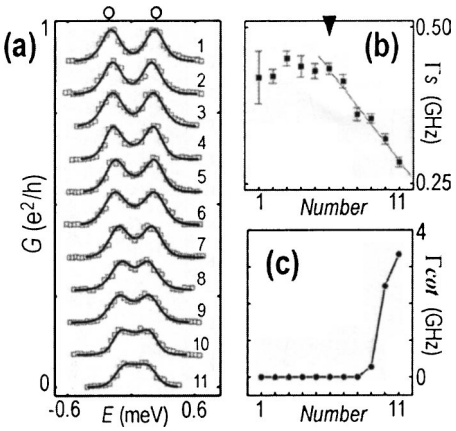

FIG. 4. (a) Single conductance traces along line γ for different interdot couplings, showing the transition from the molecular ordered state to the pseudo-Kondo regime (data open boxes; theory, solid lines). The topmost trace corresponds to Fig. 3(b), the trace labeled 6 refers to Fig. 3(a) and the lowest trace to Fig. 2(a). The line plots are displayed with an offset of $0.09e^2/h$ for clarity. (b) Fitted sequential tunneling rates Γ_S, showing a decrease for curves from 6 (black triangle) to 11 with a straight line as a guide to the eyes. (c) Fitted cotunneling rates Γ_{cot} show a rapid increase at lowest tunnel couplings.

measurement illustrates the transition between the pseudospin Kondo state and fully molecular modes inside the double quantum dot. Finally, in Fig. 3(b), all boundaries of a two-dot phase diagram are observable. Very distinct to the pseudospin Kondo regime in Fig. 2(a), also triple points appear as marked by white circles. At these points the conductance is maximum, since electrons from source can sequentially tunnel via three different double-dot ground states to drain.[16] The top curve of Fig. 4(a) with number 1 highlights a line plot from the phase diagram in Fig. 3(b) along line γ from one triple point to another. Clearly the overall increase in conductance at the triple points is seen (indicated by white circles). In between, both first- and second-order tunneling processes via states $(n,m-1)$ and $(n-1,m)$ give rise to conductance as expected for parallel quantum dots.[13] More precisely, the theory fit (solid line) which follows nicely the experimental data (open boxes) reveals that sequential tunneling events dominate this regime with $\Gamma_S = (0.42 \pm 0.04)$ GHz and $\Gamma_{\mathrm{cot}} < 1$ MHz. Curves 2–11 show the effect of a decreasing interdot coupling. As depicted by black lines, for each coupling the model successfully fits all curves. We find that the fit yields progressively smaller effective Zeeman fields t while the ground-state energies of the quantum dots stay within the experimental error. It is essential for the reliability of the fits that all fit parameters except the interdot tunneling amplitude t experience only minor variation from one fit to another. Therefore, the evolution of the fitting curves is determined by the interdot tunneling t while it yields the sequential tunneling and cotunneling rates Γ_S and Γ_{cot} [as depicted in Figs. 4(b) and 4(c)]. The cotunneling contribution to the conductance rapidly increases for the lowest tunnel couplings and is essential in order to stabilize the fit. The sequential rate Γ_S decreases towards smaller interdot couplings and shows a transition at trace number 6 (black triangle). This trace refers to the phase diagram of Fig. 3(a) which also exhibits the onset of sequential tunneling via individual dots. We explain the transition by a slight asymmetry of the tunnel couplings between each dot and the right and left leads. Assume $T_{1l}/T_{1r} = T_{2r}/T_{2l} = \lambda > 1$, where r and l denote the right and left leads and 1 and 2 the dot numbers.[21] The sequential tunneling contribution is given by the square of the smaller tunnel coupling which is proportional to $|T_{1r}|^2 + |T_{2l}|^2$. However, the cotunneling contribution is dominated by the product of the largest tunneling couplings $|T_{1l}|^2 |T_{2r}|^2$. Therefore the ratio of the resonant contributions of the cotunneling and the sequential tunneling is $\lambda^4/2$ in that case. Thus, for the lowest tunneling couplings, the triple points in the phase diagrams, which are characteristic of the sequential tunneling processes, are suppressed and we can resolve the contribution of the cotunneling processes.

SUMMARY

In summary this work covers experiment and theory on pseudospin Kondo correlations in a semiconductor double quantum dot. Cryogenic transport spectroscopy reveals the sequential and correlated tunneling of electrons through the individual dots and both dots in parallel for different interdot couplings. Following the concept of pseudospin, we develop an expression for the conductance through the parallel double quantum dot. A detailed comparison between the model and experiment reveals a crossover from a ground state with pseudospin Kondo correlations to a state with frozen pseudospin.

ACKNOWLEDGMENTS

We would like to thank J. P. Kotthaus and D. D. Awschalom for continuous support and stimulating discussions. We acknowledge financial support by the Deutsche Forschungsgemeinschaft through the Sonderforschungsbereiche (Grant Nos. SFB 348 and SFB 508) and the Schwerpunkt "Quanteninformationsverarbeitung" (Grant No. Bl/487-2-2), the Defense Advanced Research Projects Agency (EOARD project F61775-01-WE037), and the Bundesministerium fuer Wissenschaft und Technik.

*Present address: Center for Spintronics and Quantum Computation, University of California, Santa Barbara, CA 93106. Electronic address: aholleitner@iquest.ucsb.edu

[1] J. Kondo, Prog. Theor. Phys. **32**, 37 (1964).

[2] B. A. Jones, C. M. Varma, and J. W. Wilkins, Phys. Rev. Lett. **61**, 125 (1988); B. A. Jones and C. M. Varma, Phys. Rev. B **40**, 324 (1989).

[3] P. Fulde, *Electron Correlation in Molecules and Solids*, Springer

Series in Solid States Sciences (Springer, Berlin, 1995).
[4] T. K. Ng and P. A. Lee, Phys. Rev. Lett. **61**, 1768 (1988); L. I. Glazman and M. E. Raikh, JETP Lett. **47**, 452 (1988).
[5] D. Goldhaber-Gordon, H. Shtrikman, D. Mahalu, D. Abusch-Magder, and U. Meirav, Nature (London) **391**, 156 (1998); S. M. Cronenwett, T. H. Oosterkamp, and L. P. Kouwenhoven, Science **281**, 540 (1998); J. Schmid, J. Weis, K. Eberl, and K. v. Klitzing, Physica B **256**, 182 (1998); Phys. Rev. Lett. **84**, 5824 (2000).
[6] F. Simmel, R. H. Blick, J. P. Kotthaus, W. Wegscheider, and M. Bichler, Phys. Rev. Lett. **83**, 804 (1999).
[7] A. Georges and Y. Meir, Phys. Rev. Lett. **82**, 3508 (1999); H. Jeong *et al.*, Science **293**, 2221 (2001).
[8] G. Zarand, Phys. Rev. B **52**, 13 459 (1995); G. Zarand and K. Vladar, Phys. Rev. Lett. **76**, 2133 (1996); L. Borda *et al.*, *ibid.* **90**, 026602 (2003); D. Boese, W. Hofstetter, and H. Schoeller, Phys. Rev. B **66**, 125315 (2002).
[9] A. W. Holleitner, R. H. Blick, A. K. Huettel, K. Eberl, and J. P. Kotthaus, Science **297**, 70 (2002).
[10] R. H. Blick, D. Pfannkuche, R. J. Haug, K. v. Klitzing, and K. Eberl, Phys. Rev. Lett. **80**, 4032 (1998).
[11] A. W. Holleitner, C. R. Decker, H. Qin, K. Eberl, and R. H. Blick, Phys. Rev. Lett. **87**, 256802 (2001).
[12] A. W. Holleitner, R. H. Blick, H. Qin, A. K. Huettel, K. Eberl, and J. P. Kotthaus, Physica E (Amsterdam) **12**, 774 (2002).
[13] A. W. Holleitner, R. H. Blick, and K. Eberl, Appl. Phys. Lett. **82**, 1887 (2003).
[14] F. Hofmann, T. Heinzel, D. A. Wharam, and J. P. Kotthaus, Phys. Rev. B **51**, 13 872 (1995).
[15] W. G. van der Wiel, S. De Franceschi, J. M. Elzerman, T. Fujisawa, S. Tarucha, and L. P. Kouwenhoven, Rev. Mod. Phys. **75**, 1 (2003).
[16] L. P. Kouwenhoven, C. M. Marcus, P. L. McEuen, S. Tarucha, R. M. Westervelt, and N. S. Wingreen, in *Mesoscopic Electron Transport*, edited by L. L. Sohn, L. P. Kouwenhoven, and G. Schoen, Vol. 345 of *NATO Advanced Study Institute, Series E* (Kluwer, Dordrecht, 1997).
[17] C. W. J. Beenakker, Phys. Rev. B **44**, 1646 (1991).
[18] S. Sasaki, S. de Franceschi, J. M. Elzerman, W. G. Van der Wiel, M. Eto, S. Tarucha, and L. P. Kouwenhoven, Nature (London) **405**, 764 (2000).
[19] H. van Houten, C. W. J. Beenaker, and A. A. M. Staring, in *Single Charge Tunneling*, edited by H. Grabert and M. H. Devoret, Vol. 294 of *NATO Advanced Study Institute, Series B* (Plenum, New York, 1992), p. 179, Eq. (24).
[20] Filters are only integrated at room temperature.
[21] This assumption is supported by nonlinear transport measurements which are not shown here.